Cell

# Single-Stranded siRNAs Activate RNAi in Animals

Walt F. Lima,[1,*] Thazha P. Prakash,[2] Heather M. Murray,[1] Garth A. Kinberger,[2] Wenyu Li,[2] Alfred E. Chappell,[3] Cheryl S. Li,[1] Susan F. Murray,[4] Hans Gaus,[3] Punit P. Seth,[2] Eric E. Swayze,[2] and Stanley T. Crooke[1]
[1]Core Antisense Research
[2]Medicinal Chemistry
[3]Structural Biology
[4]Molecular Pharmacology
Isis Pharmaceuticals Inc., Carlsbad, CA 92010, USA
*Correspondence: wlima@isisph.com
http://dx.doi.org/10.1016/j.cell.2012.08.014

## SUMMARY

The therapeutic utility of siRNAs is limited by the requirement for complex formulations to deliver them to tissues. If potent single-stranded RNAs could be identified, they would provide a simpler path to pharmacological agents. Here, we describe single-stranded siRNAs (ss-siRNAs) that silence gene expression in animals absent lipid formulation. Effective ss-siRNAs were identified by iterative design by determining structure-activity relationships correlating chemically modified single strands and Argonaute 2 (AGO2) activities, potency in cells, nuclease stability, and pharmacokinetics. We find that the passenger strand is not necessary for potent gene silencing. The guide-strand activity requires AGO2, demonstrating action through the RNAi pathway. ss-siRNA action requires a 5′ phosphate to achieve activity in vivo, and we developed a metabolically stable 5′-*(E)*-vinylphosphonate (5′-VP) with conformation and sterioelectronic properties similar to the natural phosphate. Identification of potent ss-siRNAs offers an additional option for RNAi therapeutics and an alternate perspective on RNAi mechanism.

## INTRODUCTION

RNA interference (RNAi) is a mechanism by which double-stranded RNA triggers the loss of RNA of homologous sequence (Fire et al., 1998). Long double-strand RNAs are processed by the double-strand endonuclease Dicer into short RNA duplexes ranging from 21 to 23 nucleotides in length (Bernstein et al., 2001). The double-strand RNA-binding proteins Dicer and HIV-1 *trans*-activating response RNA-binding protein (TRBP) transfer the short RNA duplexes to the RNA-induced silencing complex (RISC) (Chendrimada et al., 2005). The antisense strand of the short RNA duplexes binds to the RISC endonuclease Argonaute 2 (Ago2), which then cleaves the target mRNA (Elbashir et al., 2001; Tomari et al., 2004; Nykänen et al., 2001; Meister et al., 2004; Rand et al., 2004; Song et al., 2004; Rivas et al., 2005).

Synthetic short interfering RNA duplexes (siRNA) have been shown to potently reduce complementary mRNA in cells by activating the RISC mechanism and show promise as therapeutic agents (Elbashir et al., 2001; Caplen, 2003). However, in their current state, the therapeutic utility of siRNA is limited by the requirement for complex lipid formulations to deliver siRNA to peripheral tissues (Vaishnaw et al., 2010). Lipid formulations of oligonucleotides and polynucleotides are complex, expensive to manufacture, and shown to be associated with proinflammatory toxicities (Tao et al., 2011). In contrast, single-strand antisense oligonucleotides do not require special formulations to distribute to peripheral tissues (Bennett and Swayze, 2010). Interestingly, although siRNAs are double-stranded structures, human Ago2 has been shown to bind only short single-stranded RNAs (ssRNA) (Lima et al., 2009a; Rivas et al., 2005). In addition, human Dicer has been shown to bind short ssRNAs with affinities comparable to siRNAs, suggesting that ssRNAs might be capable of activating the RNAi pathway (Lima et al., 2009b).

ssRNAs were shown early on to reduce complementary target RNA in cells, although the reported activities of the ssRNAs were poor compared to double-stranded siRNA (Martinez et al., 2002; Schwarz et al., 2002; Wu et al., 1998). The metabolic instability of the ssRNAs compared to double-stranded siRNAs likely contributed to the poor activities observed for the ssRNAs (Braasch et al., 2003, Wu et al., 1998). Chemical modifications predicted to enhance the nuclease stability of ssRNAs have been evaluated in cells and animals, and many of the modifications and motifs enlisted were patterned after successful siRNA motifs (Holen et al., 2003; Hall et al., 2004; Haringsma et al., 2012; Prakash et al., 2005; Dande et al., 2006; Allerson et al., 2005). These modified ssRNAs were significantly less potent than siRNAs, suggesting that the structure-activity relationships for ssRNA differ from siRNAs (Holen et al., 2003; Hall et al., 2004; Haringsma et al., 2012). In addition, absent lipid formulations, the ssRNAs were inactive in animals, suggesting that the modified ssRNAs exhibited insufficient metabolic stability and other necessary pharmacokinetic properties to support activity (Haringsma et al., 2012). Taken together, these results suggest that

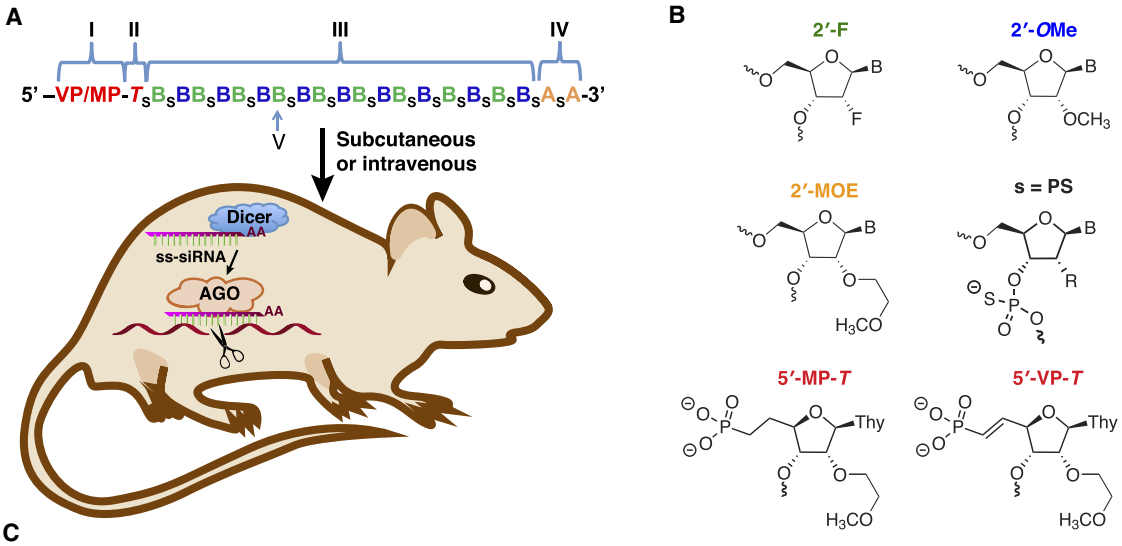


C

| ID | Structure (5'→3') | ss-siRNA $IC_{50}$ (nM) | siRNA $IC_{50}$ (nM) | ss-siRNA $t_{1/2}$ (h) |
|---|---|---|---|---|
| 1 | $P_o$-UUGUCUCUGGUCCUUACUU | ND | 0.2 ± 0.1 | 0.03 |
| 2 | $P_o$-$U_sU_sG_sU_sC_sU_sC_sU_sG_sG_sU_sC_sC_sU_sU_sA_sC_sU_sU$ | >100 | 0.5 ± 0.1 | 0.22 |
| 3 | $P_o$-$U_sU_sG_sU_sC_sU_sC_sU_sG_sG_sU_sC_sC_sU_sU_sA_sC_sU_sU$ | >100 | 0.4 ± 0.1 | 6.3 |
| 4 | $P_o$-UUGUCUCUGGUC$_sC_sU_sU_sA_sC_sU_sU$ | 39 ± 9 | 0.2 ± 0.0 | 0.12 |
| 5 | $P_o$-UUGUCUCUGGUC$_sC_sU_sU_sA_sC_sU_sU$ | 19 ± 6 | 0.2 ± 0.1 | 0.25 |
| 6 | $P_o$-UUGUCUCUGGUCCU$_sU_sA_sC_sU_sU_sA_sA$ | 5 ± 2 | 0.2 ± 0.1 | 0.32 |
| 7 | $P_o$-$U_sU$GUCUCUGGUC$_sC_sU_sU_sA_sC_sU_sU_sA_sA$ | 3 ± 1.2 | 0.2 ± 0.1 | >8 |
| 8 | $P_o$-$T_sU_sG$U$_sC$U$_sC$U$_sG$G$_sU$C$_sC$U$_sU_sA_sC_sU_sU_sA_sA$ | 2 ± 0.4 | 0.2 ± 0.1 | >8 |

**Figure 1. Modified Nucleic Acid Composition, In Vitro Potencies, and Half-Lives of Potent ss-siRNAs**

(A) Configuration of the optimized chemically modified ss-siRNA includes: metabolically stable 5′ phosphonate analog (I); 2′-MOE-modified 5′-terminal nucleotide for protection from 5′ exonuclease activity (II); alternating 2′-F and 2′-OMe motifs with contiguous PS modifications at the 3′ pole and alternating PS and PO motifs at the 5′ pole of the ss-siRNA for protection from endonuclease activity (III); 2′-MOE-modified adenosine dinucleotide at the 3′ terminus for protection from 3′ exonuclease activity and enhanced potency (IV); and C16 modification for enhanced tissue distribution (V). The color coding of the modified nucleotides is as described in (B). Following either subcutaneous or intravenous administration, the ss-siRNA distributed to peripheral tissues and engaged the RNAi mechanism to degrade the target mRNA.

(B) Nucleotide modifications include: phosphorothioate (PS), 2′-fluororibose (green, 2′-F), 2′-methoxyribose (blue, 2′-OMe), 2′-methoxyethylribose (orange, 2′-MOE), 5′-methylenephosphonate (red, 5′-MP), 5′-*(E)*-vinyl-phosphonate (red, 5′-VP), C10 ($T_{C10}$), and C16 ($T_{C16}$).

(C) Nucleotide modifications are described in (B). The siRNAs were prepared using a complementary RNA sense strand (5′-AAGUAAGGACCAGAGACAA-3′). The in vitro potencies ($IC_{50}$) correspond to the ss-siRNA or siRNA concentration, resulting in 50%reduction of the PTEN mRNA level compared to lipid-only treated cells. Data are represented as mean ± SD. The metabolic half-lives ($t_{1/2}$) of the ss-siRNAs are defined as the incubation time in primary hepatocyte homogenates, resulting in 50% loss of the full-length ss-siRNA. ND, not determined.

See also Table S1 and Figures 1 and 5.

to develop potent ssRNA therapeutics requires: (1) the identification of chemical modifications that enhance the metabolic stability and other pharmacokinetic properties of the ssRNAs and (2) interactions with key components of the RISC mechanism.

In this study, we evaluated the abilities of chemically modified single-stranded short interfering RNA (ss-siRNA) molecules to bind to human Ago2 and support cleavage activity (Figure 1A). Having defined the sites that tolerate modifications and the structure-activity relationships of productive interactions with Ago2, we then evaluated the modified ss-siRNAs for stability, other pharmacokinetic properties, and activity in cultured cells. Next, the optimized ss-siRNAs were evaluated in animals. We demonstrated that optimized ss-siRNAs could be designed to reduce multiple targets and could work in the liver and other tissues after subcutaneous or intravenous dosing and confirmed that the observed activities were RISC mediated.

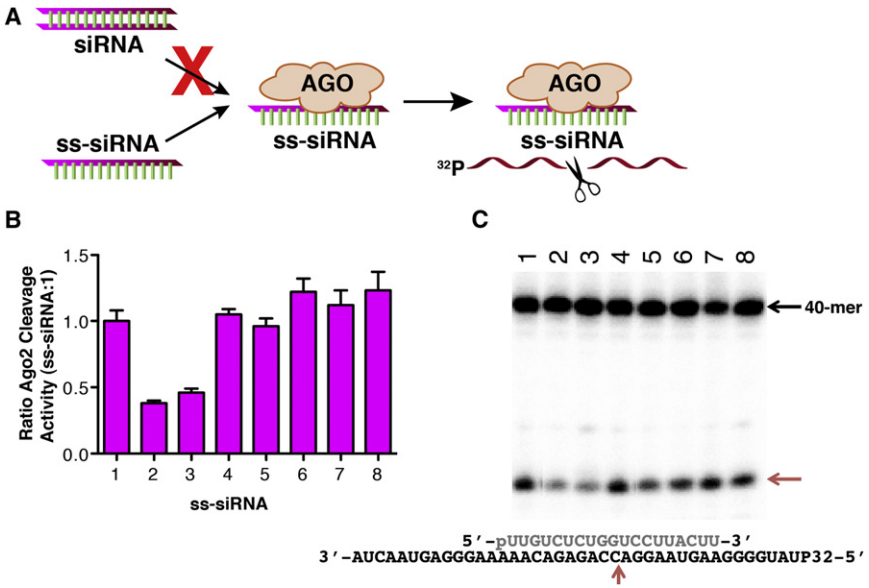


**Figure 2. Ago2 Cleavage Activities of Chemically Modified ss-siRNAs**

(A) Scheme for cleavage of ss-siRNA by Ago2. The ss-siRNA was bound to the enzyme prior to adding the target RNA. Ago2 containing the ss-siRNA was incubated with the $^{32}$P-labeled target RNA. Double-stranded siRNAs were not tested, as they do not bind recombinant human Ago2.

(B) Relative recombinant human Ago2 cleavage activity for various ss-siRNAs. Cleavage activities of the ss-siRNAs are reported as a ratio of the cleavage activity observed for the unmodified ss-siRNA1. Data are represented as mean ± SD.

(C) PAGE analysis of $^{32}$P-labeled 40 nucleotide target RNA and human Ago2 cleavage products (red arrow). The position of the Ago2 cleavage site (red arrow) in the target RNA (black sequence) is shown relative to the ss-siRNA (gray sequence).

## RESULTS

### Identification of Potent and Metabolically Stable ss-siRNAs

To identify potent ss-siRNA molecules, we determined the metabolic stabilities of the ss-siRNAs in cell homogenates and the potencies of the ss-siRNAs and corresponding siRNAs in cells. We also measured cleavage activities of purified recombinant human Ago2 bound to the ss-siRNAs in order to better understand the structure-activity relationships between the ss-siRNA and Ago2. Human Ago2 cleavage activities were not determined for siRNAs, as the enzyme has been shown not to bind double-stranded siRNA (Figure 2A) (Lima et al., 2009a; Rivas et al., 2005).

First, we evaluated ss-siRNAs containing uniform phosphorothioate intranucleotide linkages (PS), as phosphorothioates have been shown to enhance both metabolic stability and pharmacokinetic properties of single-stranded antisense oligonucleotides (Figure 1B) (Graham et al., 1998; Graham et al., 2001). The uniform PS substitutions enhanced the metabolic stability of the ss-siRNAs compared to the unmodified ss-siRNA 1, and in the case of the 2′-F ss-siRNA 3, the half-life in hepatocyte homogenates exceeded 6 hr (Figure 1C). Unfortunately, the ss-siRNAs containing uniform PS substitutions (2 and 3) were inactive in cells and exhibited reduced human Ago2 cleavage activities (Figures 1C, 2B, and 2C). The siRNA analogs of the ss-siRNAs 2 and 3 were also less potent in vitro when compared to the unmodified ss-siRNA 1 (Figure 1C).

A survey of the preferred sites for PS substitutions in the ss-siRNA identified an active motif consisting of seven contiguous PS substitutions positioned at the 3′ pole of the ss-siRNA (4 and 5) (Figure 1C). The siRNAs (4 and 5) were also more active compared to the uniform PS-modified siRNAs (2 and 3) (Figure 1C). Similarly, enhanced human Ago2 cleavage activities were observed for ss-siRNAs 4 and 5 compared to the ss-siRNAs 2 and 3 (Figures 2 B and 2C). The ss-siRNA containing the uniform 2′-F and seven PS motif (5) exhibited the greatest in vitro potency ($IC_{50}$ of 19 nM) (Figure 1C).

To further enhance the potency of the ss-siRNA 5, we turned our attention to the 3′ terminus of the compound. Previous reports indicated that single-stranded 3′-dinucleotide overhangs containing purine residues enhance the in vitro potencies of siRNAs presumably by interacting with human Dicer (Rose et al., 2005; Lima et al., 2009b).

To determine whether a similar dinucleotide composition at the 3′ terminus would enhance the in vitro potency of ss-siRNAs, two adenosine nucleotides were appended to the 3′ terminus of the ss-siRNA containing the uniform 2′-F, seven PS ss-siRNA motif (6) (Figure 1C). A 4-fold increase in potency was observed for the ss-siRNA 6 containing the additional 2′-MOE adenosine dinucleotide compared to the ss-siRNA 5 without the additional 3′-dinucleotide (Figure 1C). Importantly, similar human Ago2 cleavage activities were observed for the ss-siRNAs 5 and 6, suggesting that Ago2 was not contributing significantly to the enhanced potency observed for the ss-siRNA 6 (Figures 2B and 2C).

Similar half-lives were observed for the ss-siRNAs 5 and 6 in hepatocyte homogenates, suggesting that the 2′-MOE modified adenosine dinucleotide had little effect on nuclease stability of these ss-siRNAs (Figure 1C). The LC-MS analysis showed that the majority of the nuclease degradation occurred in the non-phosphorothioate region, i.e., the 5′ pole, of the ss-siRNA 5 (Figure 3A). These data suggest that, although the seven contiguous phosphorothioates were sufficient to protect the 3′ pole of the ss-siRNA from nuclease degradation in hepatocyte homogenates, additional chemical modification of the 5′ pole of the ss-siRNA was required to further improve the metabolic stability of the ss-siRNA.

An alternating 2′-F and 2′-methoxy ribonucleotide (2′-OMe) motif was employed, as similar motifs were reported to enhance the potency and metabolic stability of siRNAs (Figure 1B) (Allerson et al., 2005; Dande et al., 2006; Prakash et al., 2005). Additional phosphorothioate substitutions were also included along

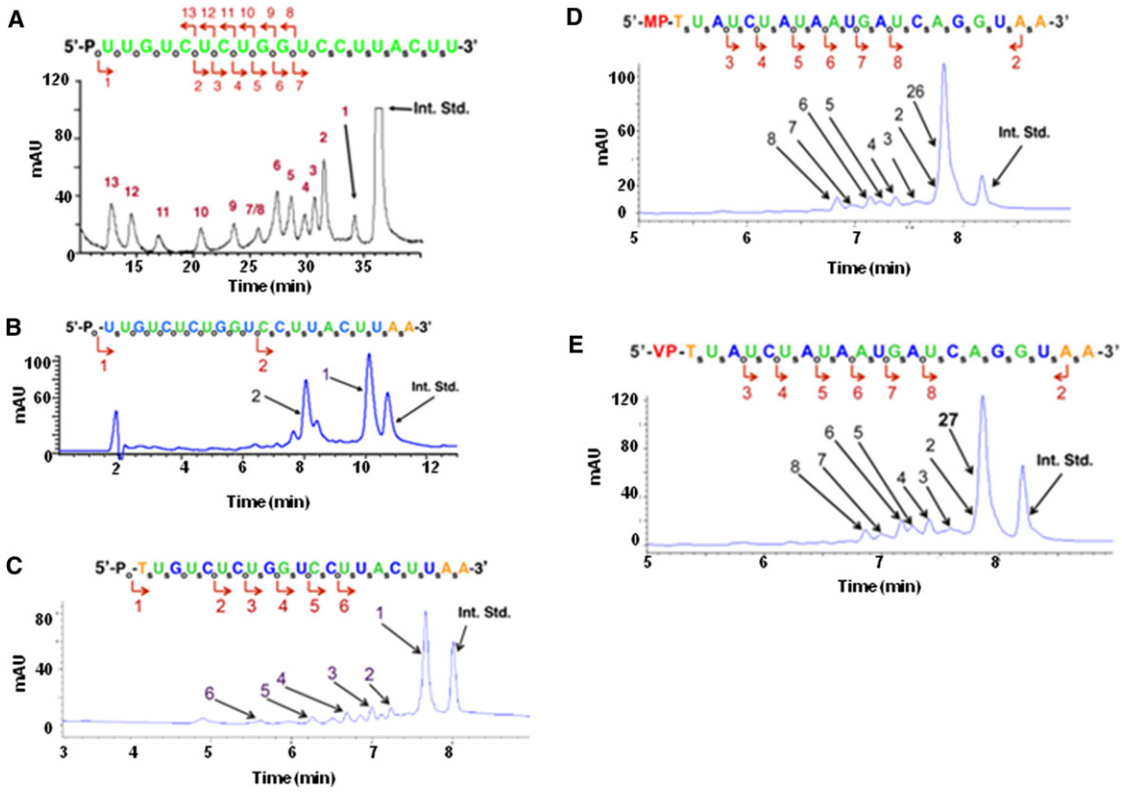


**Figure 3. Identification of ss-siRNA Metabolites Extracted from Hepatocyte Homogenates or Mouse Liver**

(A) Liquid chromatography-tandem mass spectrometry (LC-MS) analysis of the ss-siRNA 5 extracted from hepatocyte homogenates 1 hr posttreatment. (B–E) LC-MS of ss-siRNAs 7 (B), 8 (C), 26 (D), and 27 (E) extracted from mouse liver 48 hr posttreatment. The liquid chromatography profiles show the relative abundance of the metabolites identified by mass spectrometry compared to the internal standard (Int. Std.). Numbered arrows indicate the position of degradation sites in the ss-siRNA in relationship to the corresponding peaks from the liquid chromatography profile.

with either a 2′-OMe (7) or 2′-MOE (8) at the 5′ terminus. A significant increase in metabolic stability was observed for the ss-siRNAs 7 and 8 with half-lives in hepatocyte homogenates greater than 8 hr (Figure 1C). An ~2-fold increase in potency was observed for the ss-siRNAs 7 and 8 compared to the ss-siRNA 6 (Figure 1C). The alternating 2′-F and 2′-OMe motif appeared to be well tolerated by human Ago2, as similar cleavage activities were observed for the ss-siRNAs 7 and 8 compared to the unmodified ss-siRNA 1 (Figure 2B and C). Similarly, the in vitro potencies observed for the siRNAs 7 and 8 were comparable to the unmodified siRNA 1 (Figure 1C). Importantly, we identified ss-siRNAs that are both potent and metabolically stable in vitro.

## ss-siRNA Activity Is Ago2 Dependent

To determine whether ss-siRNA-mediated reduction of the target mRNA in cells was the result of Ago2 cleavage, we performed 5′ rapid amplification of cDNA ends (5′-RACE) to map the cleavage site on the PTEN mRNA from lipid-only-treated cells and cells treated with the ss-siRNA 8 (Figure 4A). Consistent with the Ago2 cleavage mechanism, sequencing analysis of the 5′-RACE products revealed a single cleavage site positioned at the phosphodiester bond bridging the ribonucleotides opposing the tenth and eleventh nucleotide from the 5′ terminus of the ss-siRNA (Figure 4A). No cleavage products were observed for the lipid-only-treated cells (data not shown). Taken together, these data suggest that ss-siRNAs activate Ago2 to degrade the target mRNA in a manner similar to that reported for siRNAs (Elbashir et al., 2001; Tomari et al., 2004; Nykänen et al., 2001; Meister et al., 2004; Rand et al., 2004; Song et al., 2004; Rivas et al., 2005).

To confirm that ss-siRNAs function through an Ago2 mechanism, we measured the potency of ss-siRNA 8 and corresponding siRNA in wild-type and Ago2 knockout mouse embryonic fibroblast (MEF) cells (Figure 4C). Both the ss-siRNA 8 and siRNA showed dose-dependent reduction of the PTEN mRNA in the wild-type MEF cells (Figure 4C). However, no PTEN mRNA reduction was observed for either the 8 ss-siRNA or siRNA in the Ago2 knockout cells, suggesting that the activities of ss-siRNA and siRNA are Ago2 dependent (Figure 4C).

## The 5′ Phosphate Is Required for ss-siRNA Activity, but Not for siRNA Activity

Previous reports suggest that the 5′ phosphate is important for siRNA and ss-siRNA activity and enhance the binding affinity of ss-siRNAs to human Ago2 (Chen et al., 2008; Haringsma et al., 2012; Lima et al., 2009a). To evaluate the role of the 5′ phosphate in the activities of the ss-siRNAs, we determined

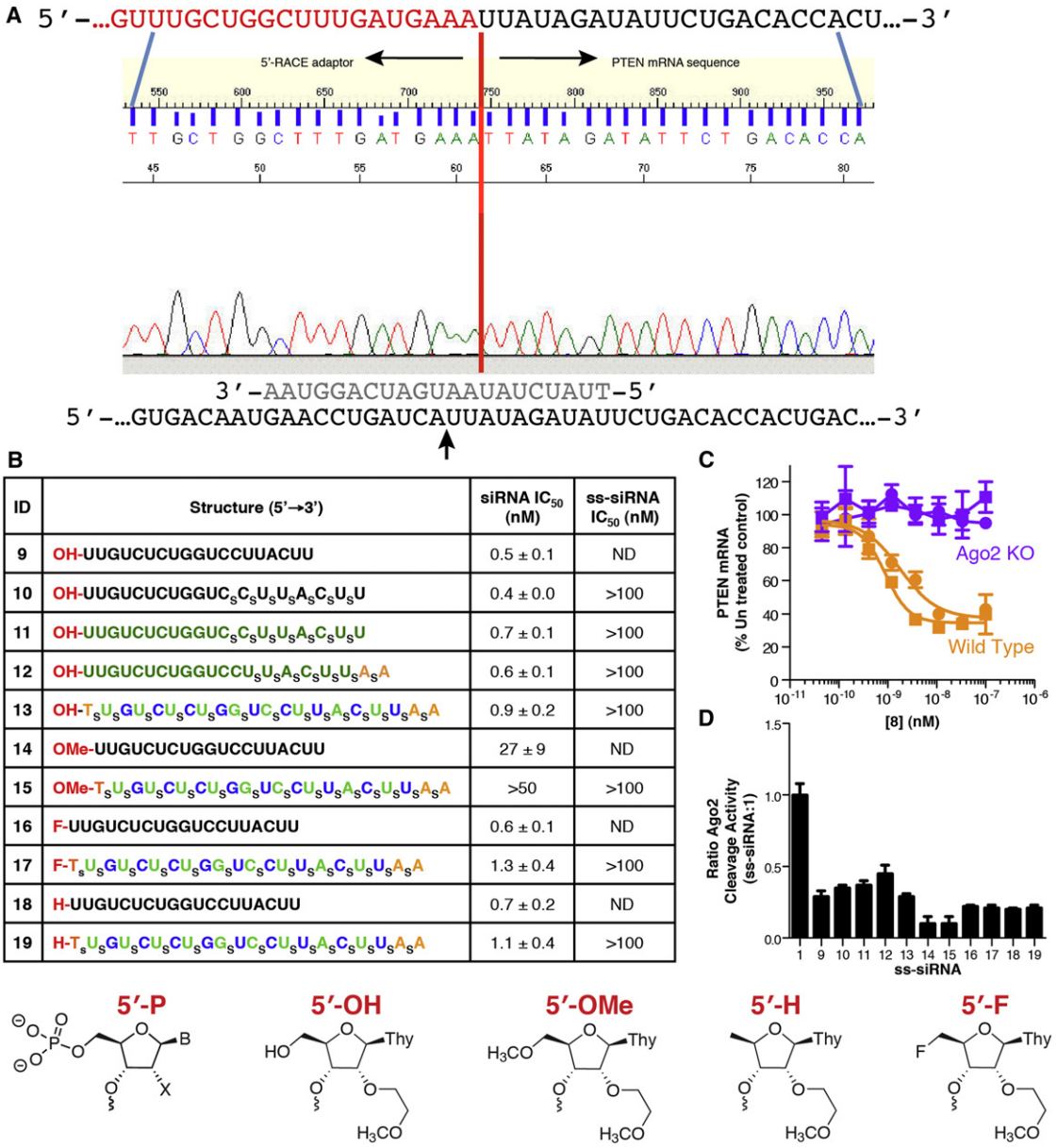


| ID | Structure (5′→3′) | siRNA $IC_{50}$ (nM) | ss-siRNA $IC_{50}$ (nM) |
|---|---|---|---|
| 9 | OH-UUGUCUCUGGUCCUUACUU | 0.5 ± 0.1 | ND |
| 10 | OH-UUGUCUCUGGUC$_S$C$_S$U$_S$U$_S$A$_S$C$_S$U$_S$U | 0.4 ± 0.0 | >100 |
| 11 | OH-UUGUCUCUGGUC$_S$C$_S$U$_S$U$_S$A$_S$C$_S$U$_S$U | 0.7 ± 0.1 | >100 |
| 12 | OH-UUGUCUCUGGUCCU$_S$U$_S$A$_S$C$_S$U$_S$U$_S$A$_S$A | 0.6 ± 0.1 | >100 |
| 13 | OH-T$_S$U$_S$G$_S$U$_S$C$_S$U$_S$C$_S$U$_S$G$_S$G$_S$U$_S$C$_S$C$_S$U$_S$U$_S$A$_S$C$_S$U$_S$U$_S$A$_S$A | 0.9 ± 0.2 | >100 |
| 14 | OMe-UUGUCUCUGGUCCUUACUU | 27 ± 9 | ND |
| 15 | OMe-T$_S$U$_S$G$_S$U$_S$C$_S$U$_S$C$_S$U$_S$G$_S$G$_S$U$_S$C$_S$C$_S$U$_S$U$_S$A$_S$C$_S$U$_S$U$_S$A$_S$A | >50 | >100 |
| 16 | F-UUGUCUCUGGUCCUUACUU | 0.6 ± 0.1 | ND |
| 17 | F-T$_S$U$_S$G$_S$U$_S$C$_S$U$_S$C$_S$U$_S$G$_S$G$_S$U$_S$C$_S$C$_S$U$_S$U$_S$A$_S$C$_S$U$_S$U$_S$A$_S$A | 1.3 ± 0.4 | >100 |
| 18 | H-UUGUCUCUGGUCCUUACUU | 0.7 ± 0.2 | ND |
| 19 | H-T$_S$U$_S$G$_S$U$_S$C$_S$U$_S$C$_S$U$_S$G$_S$G$_S$U$_S$C$_S$C$_S$U$_S$U$_S$A$_S$C$_S$U$_S$U$_S$A$_S$A | 1.1 ± 0.4 | >100 |

**Figure 4. ss-siRNA Activity Is Ago2 Dependent and Requires a 5′ Phosphate**

(A) The position of the cleavage site within the PTEN mRNA from cells treated with ss-siRNA 8 was determined using 5′-RACE. Sequencing results are shown in the top panel. The red sequence corresponds to the 5′-RACE adaptor and the black sequence to the downstream cleavage product of the PTEN mRNA. The position of cleavage is identified as the junction between the 5′-RACE adaptor and the PTEN mRNA (red line). The sequence below shows the position of cleavage site (arrow) on the PTEN mRNA (black sequence) in relation to the hybridization site for the ss-siRNA (gray sequence).

(B) 5′-terminal modifications include: 5′ phosphate (5′-P), 5′ hydroxyl (5′-OH), 5′ methoxy (5′-OMe), 5′ deoxy (5′-H), and 5′ fluoro (5′-F). The siRNAs were prepared and the in vitro potencies in HeLa cells reported as in Figure 1. ND, not determined.

(C) Dose-dependent reduction of PTEN mRNA from wild-type (gold) and Ago2 knockout (blue) mouse embryonic fibroblast cells (MEF) transfected with the ss-siRNA 8 (solid circle) or corresponding siRNA (solid square). PTEN mRNA levels are reported as a percentage of the PTEN mRNA levels for the lipid-only-treated cells.

(D) Human Ago2 cleavage activities of ss-siRNA are reported as described in Figure 2.

See also Table S1 and Figures S2, S3, and S4. Data are represented as mean ± SD.

the Ago2 cleavage activities of ss-siRNAs and corresponding siRNAs containing a 5′-hydroxyl (5′-OH) moiety (Figures 4B and 4D). The ss-siRNAs containing the 5′-OH (9 through 13) exhibited human Ago2 cleavage activities that were 2- to 4-fold lower than the corresponding ss-siRNAs containing a 5′-phosphate (1, 4, 5, and 8) (Figures 1C and 4B). A similar 2- to 4-fold

A

| | ID | Structure (5'→3') | Hepatocyte $IC_{50}$ ($\mu$M) |
|---|---|---|---|
| I | 7 | $P_o$-$U_sU_GU_CU_CU_GG_UC_sC_sU_sU_sA_sC_sU_sU_sA_sA$ | 3 |
| | 8 | $P_o$-$T_sU_sG_UC_sU_sC_sU_sG_GG_UC_sC_sU_sU_sA_sC_sU_sU_sA_sA$ | 1 |
| | 20 | MP-$T_sU_sG_UC_sU_sC_sU_sG_GG_UC_sC_sU_sU_sA_sC_sU_sU_sA_sA$ | 15 |
| | 21 | VP-$T_sU_sG_UC_sU_sC_sU_sG_GG_UC_sC_sU_sU_sA_sC_sU_sU_sA_sA$ | 11 |
| | 22 | $P_o$-$T_sG_sA_AC_sA_sU_UG_GG_sA_AG_sA_sG_sU_sU_sU_sC_sA_sA$ | 1 |
| | 23 | MP-$T_sG_sA_AC_sA_sU_UG_GG_sA_AG_sA_sG_sU_sU_sU_sC_sA_sA$ | 13 |
| | 24 | VP-$T_sG_sA_AC_sA_sU_UG_GG_sA_AG_sA_sG_sU_sU_sU_sC_sA_sA$ | 4 |
| | 25 | $P_o$-$T_sU_sA_UC_sU_sA_UA_sA_sU_GG_sA_sU_sC_sA_sG_sG_sU_sA_sA$ | 1 |
| | 26 | MP-$T_sU_sA_UC_sU_sA_UA_sA_sU_GG_sA_sU_sC_sA_sG_sG_sU_sA_sA$ | 7 |
| | 27 | VP-$T_sU_sA_UC_sU_sA_UA_sA_sU_GG_sA_sU_sC_sA_sG_sG_sU_sA_sA$ | 1 |
| | 28 | VP-$T_sU_sA_UC_sU_sAT_{C10S}A_sA_sU_GG_sA_sU_sC_sA_sG_sG_sU_sA_sA$ | 2 |
| | 29 | VP-$T_sU_sA_UC_sU_sAT_{C16S}A_sA_sU_GG_sA_sU_sC_sA_sG_sG_sU_sA_sA$ | 10 |
| | 30 | VP-$T_sA_sU_CA_sA_sU_CG_sU_sA_sU_GG_sG_sU_sU_sA_sA_sA_sA$ | >100 |
| II | 31 | VP-$T_sU_sA_AG_sA_sC_sU_GG_sA_GG_sA_sU_sG_sA_sU_sC_sC_sA_sA$ | 2 |
| III | 32 | VP-$T_sA_sT_GG_sA_GG_sA_AC_sA_sT_sA_sC_sT_sT_sT_sC_sC_sC_sA_sA$ | 2 |

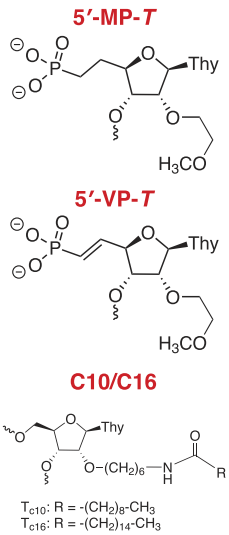


**Figure 5. Potency of ss-siRNA in Hepatocytes and Efficacy in Mice**

(A) The in vitro potencies ($IC_{50}$) of the ss-siRNAs targeting PTEN (I), Factor VII (II), or ApoCIII (III) mRNAs were determined using primary hepatocytes.

(B) The PTEN mRNA levels from the livers of mice treated with either 300 mg/kg (back bars) or 100 mg/kg (red bars) of the ss-siRNAs are reported as a percentage of the PTEN mRNA from the saline-treated group. The Factor VII (blue bar) or ApoCIII (green bar) mRNA levels from the livers of mice treated with 300 mg/kg of the Factor VII or ApoCIII ss-siRNAs, respectively.

(C) Liver concentrations of the PTEN ss-siRNAs were measured from mice treated with either 300 mg/kg (black bars) or 100 mg/kg (red bars). Liver concentrations of the Factor VII (blue bar) or ApoCIII (green bar) ss-siRNAs were measured from mice treated with 300 mg/kg.

ND and I indicate not determined and inactive, respectively. Data are represented as mean ± SD. See also Tables S1 and S2.

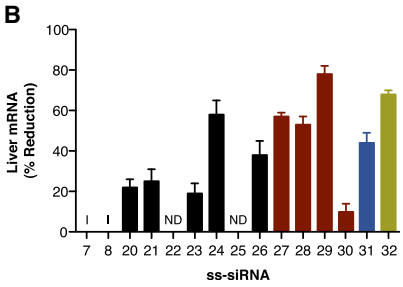


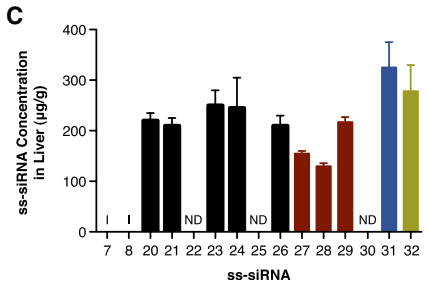


reduction in in vitro potency was observed for the siRNAs 9 through 13 compared to siRNAs 1, 4, 5, and 8 (Figures 1C and 4B). No reduction of PTEN mRNA was observed in cells treated with the modified ss-siRNAs 10 through 13, suggesting that the 5′ phosphate is required for ss-siRNA activity, but not for siRNA activity, in cells (Figure 4B).

Chen et al. used 5′-methoxy (5′-OMe)-modified siRNA to conclude that the in vitro activities of siRNAs containing a 5′ hydroxyl might be due to the 5′ phosphorylation of the siRNA in the cells, as siRNA containing 5′-OMe modification, which is refractory to phosphorylation, was inactive (Chen et al., 2008). To determine whether ss-siRNA behave in a similar manner, we designed ss-siRNAs 14 and 15 containing the 5′-OMe modification, and consistent with their results, the ss-siRNAs and siRNAs 14 and 15 were significantly less potent in vitro (Figures 4B, S1, and S2). However, the ss-siRNAs 14 and 15 were also inactive in the human Ago2 cleavage assay (Figure 4D). Taken together, our results suggest that the loss in activity observed for the siRNA containing the 5′-OMe is not due to the inability of the siRNA to be phosphorylated in the cell but that the 5′-OMe modification most likely interferes with the interaction between the ss-siRNA and Ago2 (Figures 4B and 4D).

Next, we evaluated other 5′ modifications that are refractory to phosphorylation (e.g., 5′-fluoro [5′-F] or 5′-deoxy [5′-H]) (Figures 4B, S1, S3, and S4). The human Ago2 cleavage activities observed for the ss-siRNAs containing the 5′-F (16 and 17) and 5′-H (18 and 19) moieties were comparable to the corresponding ss-siRNAs containing the 5′ hydroxyl (9 and 13), suggesting that the 5′-F and 5′-H modifications do not interfere with the interaction between the ss-siRNA and Ago2 (Figure 4D). Importantly, unlike the siRNAs containing the 5′-OMe modification (14 and 15), the siRNAs containing the 5′-F (16 and 17) and 5′-H (18 and 19) were significantly more potent even though these modifications are also refractory to phosphorylation (Figure 4B). On the other hand, the modified ss-siRNAs containing either the 5′-F (17) or 5′-H (19) were inactive in vitro (Figure 4B). Taken together, these results unequivocally demonstrate that the 5′ phosphate is required for ss-siRNA activity, but not for siRNA activity, in cells.

## 5′ Phosphate Is a Critical Determinant for ss-siRNA Activity In Vivo

The ss-siRNAs exhibiting the greatest in vitro potency and metabolic stability (7 and 8) were evaluated in primary hepatocytes and in mice (Figures 5A and 5B). In addition, the ss-siRNAs were extracted from the liver to determine the total liver concentrations of the compounds and to identify any metabolites (Figures 3B, 3C, and 5C).

No reduction in the PTEN mRNA levels was observed in mice treated with the ss-siRNAs 7 and 8 compared to the control mice (Figure 5B). Analysis of the ss-siRNAs extracted from the mouse liver revealed no intact compound (Figure 3B and C). The predominant metabolite observed for the ss-siRNA 7 consisted of the 3′ pole of the ss-siRNA containing the nine contiguous phosphorothioates (Figure 3B). Conversely, the predominant metabolite identified for the ss-siRNA 8 consisted of the full-length compound absent the 5′ phosphate, and studies with shorter

treatment times indicated that the compound was completely dephosphorylated in as few as 6 hr (Figure 3C and data not shown). Importantly, these results indicated that the 5′-terminal 2′-MOE and alternating PS substitutions at the 5′ pole significantly enhanced the metabolic stability of the ss-siRNA 8 compared to the ss-siRNA 7 in vivo (Figures 3B and 3C). In addition, the lack of in vivo activity observed for the ss-siRNA 8 was consistent with our observations that the 5′ phosphate is required for ss-siRNA activity. These data suggest that hepatocyte homogenates appear to be poor predictors of the metabolic stability and phosphatase activity in animals, as no measurable difference in metabolic stability was observed for the 7 and 8 ss-siRNAs in homogenates (Figure 1C).

## Identification of ss-siRNA Exhibiting Robust Activity in Animals via RNAi

Our in vitro and mechanistic studies showed that ss-siRNA activity requires a phosphate at the 5′ terminus (Figures 4B and 4D). Given that the modified ss-siRNA extracted from liver was rapidly dephosphorylated, we concluded that the loss of the phosphate was responsible for the observed lack of in vivo activity (Figures 3B, 3C, 5B). This prompted the search for 5′ phosphate analogs that are stable in animals and resulted in the identification of the 5′-methylenephosphonate (5′-MP) (Figures 1B and S1). This modification contains a phosphorous carbon bond instead of the phosphorous oxygen bond found in natural phosphates, and as there are no known natural enzymes capable of cleaving the phosphorous carbon bond, the 5′-MP modification was predicted to be stable in animals. The ss-siRNA containing the 5′-MP modification (20) was active in mice exhibiting a 22% reduction of the PTEN mRNA in liver (Figure 5B). The LC-MS analysis of the ss-siRNA 20 extracted from liver showed that the compound contained the 5′-MP moiety (Figure 3D). Importantly, these results demonstrated the reduction of target mRNA in vivo using an ss-siRNA administered without lipid formulation or sense strand. In addition, these results further demonstrated the requirement of the 5′ phosphate for ss-siRNA activity in both cells and animals.

To ensure that the activities observed for the 5′-MP ss-siRNA were not unique to this sequence, two additional target sites within the PTEN mRNA (22 and 25) were identified (Figure 5A). The 5′-MP analogs of these ss-siRNAs (23 and 26) exhibited comparable and greater in vivo activity, respectively (Figure 5B). Similar liver concentrations were observed for the ss-siRNAs 20, 23, and 26 (e.g., 220, 250, and 210 μg/g, respectively), suggesting that the greater in vivo activity observed for the ss-siRNA 26 was not due to differences in the pharmacokinetic properties of the compounds (Figure 5C). Consistent with the in vivo activities, the ss-siRNA 26 exhibited a 2-fold greater potency in vitro compared to the ss-siRNAs 20 and 23 (Figure 5A).

The reduced in vitro potency observed for the 5′-MP modified ss-siRNAs compared to the corresponding ss-siRNAs containing a 5′ phosphate may have been due to conformational and/or sterioelectronic differences between the methylenephosphonate and natural phosphate (Figure 5A). A survey of methylenephosphonate analogs identified the 5′-*(E)*-vinylphosphonate (5′-VP), which contains a double bond between 5′ and 6′ carbon in a trans configuration producing a conformation and sterioelectronic properties closer to the natural phosphate (Figures 1B and S1).

The ss-siRNAs 24 and 27 containing the 5′-VP modification exhibited comparable potencies to the ss-siRNA containing the 5′ phosphate (25) and 3- to 7-fold greater potency in vitro compared to the ss-siRNAs 23 and 26 containing the 5′-MP (Figure 5A). Consistent with the increased in vitro potency, the ss-siRNAs 24 and 27 were also more effective in vivo than the 5′-MP ss-siRNAs (Figure 5B). Again, LC-MS analysis of the ss-siRNA 27 extracted from liver showed that the compound contained the 5′-VP moiety and similar liver concentrations compared to the 5′-MP modified ss-siRNAs, suggesting that the enhanced in vivo activities observed for the 5′-VP ss-siRNAs was not due to differences in pharmacokinetic properties of the compounds (Figures 3E and 5C). Next, we determined the in vivo potency of ss-siRNA 27 (Figure 6B). The ss-siRNA 27 reduced the PTEN mRNA in a dose-dependent manner (Figure 6B).

To demonstrate that the in vivo activities observed for the ss-siRNA 27 involved an Ago2 mechanism, 5′-RACE was performed on the RNA extracted from the livers of the mice treated with the ss-siRNA 27 (Figure 6A). Similar to the in vitro 5′-RACE results, sequencing analysis of the 5′-RACE products from mice treated with the ss-siRNA 27 showed that the predominant cleavage product within the PTEN mRNA was consistent with the Ago2 cleavage mechanism, and no cleavage products were observed for the control mice (Figure 6A).

Next, we investigated the duration of action and elimination half-life of the ss-siRNA 27 in mouse liver (Figures 6C and 6D). The in vivo efficacy of the ss-siRNA 27 over time correlated with the concentrations of the ss-siRNA in the liver, with an ~60% reduction in PTEN mRNA observed by 24 hr. This was maintained for about 3 days, after which the ss-siRNA concentration in the liver declined, as did the observed activity (Figures 6C and 6D).

## ss-siRNA In Vivo Activity Is General for Other Targets

We evaluated the in vitro and in vivo activities of the 5′-VP modified ss-siRNAs targeting factor VII and ApoCIII mRNAs (Figure 5A). Potent 5′-VP ss-siRNA sequences targeting Factor VII (31) and ApoCIII (32) mRNAs identified in mouse hepatocytes were tested in mice and showed a >50% reduction of their respective target mRNAs in liver compared to the control mice (Figures 5A and 5B). The additional targets also provided the opportunity to access the target specificity of the ss-siRNAs. Specifically, we measured the PTEN and Factor VII mRNA levels for the mice treated with the ApoCIII ss-siRNA, the PTEN and ApoCIII mRNA levels for the mice treated with the Factor VII ss-siRNAs, and the ApoCIII and Factor VII mRNA levels for the PTEN ss-siRNA treated mice (Figure 6E). The ss-siRNAs reduced the levels of their respective target mRNAs, but not the off-target mRNAs (Figure 6E). A scrambled sequence control ss-siRNA (30) was also evaluated, exhibiting no reduction on PTEN mRNA in cells and a less <10% percent reduction of PTEN mRNA in mice (Figures 5A and 5B).

## Lipid Modification Improves ss-siRNA Potency in Animals

Previous studies have shown that adding lipophilic modifications can enhance distribution to the liver and cellular uptake (Crooke,

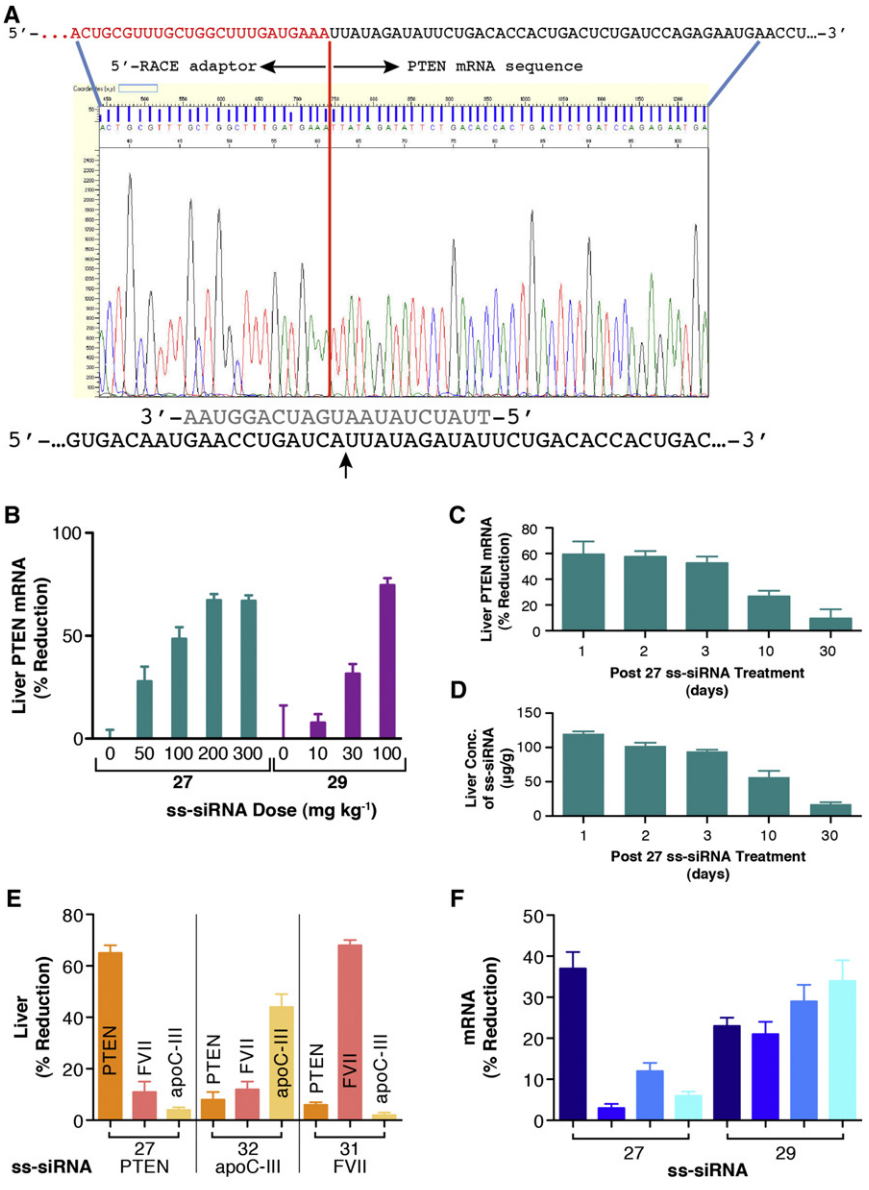


**Figure 6. In Vivo Activities of Modified ss-siRNAs following Single-Dose Administration**

(A) The position of the cleavage site within the PTEN mRNA from mice treated with the ss-siRNA 27 was determined using 5′-RACE. The procedure and interpretation of the results are as described in Figure 4A.

(B) Dose-dependent reduction of PTEN mRNA from liver of mice (n = 4) treated with a single dose of either ss-siRNAs 27 (green bars) or 29 (purple bars) administered subcutaneously and sacrificed 48 hr posttreatment.

(C and D) Duration of action (C) and tissue half-life (D) of the ss-siRNA 27 in mouse liver. Mice (n = 4) were treated with 100 mg/kg ss-siRNA 27 by subcutaneous administration and sacrificed at 1, 2, 3, 10, and 30 days posttreatment. Liver PTEN mRNA levels (C) are reported as a percentage of the PTEN mRNA levels for the saline-treated control group and the ss-siRNA 27 concentrations in the liver (D) for each time point.

(E) On- and off-target activities from livers of the mice treated with 300 mg/kg of the ss-siRNAs targeting PTEN (27), Factor VII (31), or ApoCIII (32). The PTEN (gold bar), Factor VII (tan bar), and ApoCIII (peach bar) mRNA levels were determined for all ss-siRNA-treated mice and reported as a percentage of the respective mRNAs levels from the saline-treated group.

(F) Reduction of PTEN mRNA from the peripheral tissues of mice treated with 100 mg/kg of the ss-siRNAs 27 or 29. The PTEN mRNA levels from kidney (dark blue), quadriceps (medium blue), lung (light blue), and fat (light green).

Data are represented as mean ± SD.

2008). We evaluated a number of lipophilic modifications at various positions on the ss-siRNA and identified the C10 and C16 modification, which when positioned at the eighth nucleotide from the 5′ terminus of the 5′-VP-modified ss-siRNA (28 and 29, respectively), resulted in in vitro potencies comparable to the unconjugated ss-siRNA (27) (Figures 1B, 5A, S1, and S5). In the case of the ss-siRNA 28 containing the C10 adduct, neither an increase in the liver concentrations of the ss-siRNA nor an increase in in vivo efficacy was observed compared to the unconjugated ss-siRNA 27 (Figures 5B and 5C). In contrast, the ss-siRNA containing the C16 modification (29) exhibited greater in vivo activity and liver concentration compared to the unconjugated ss-siRNA (Figures 5B and 5C). Greater activity was also observed for the ss-siRNA 29 containing the C16 modification in quadriceps, lung, and fat tissues compared to the ss-siRNA 27, suggesting that the C16 adduct appeared to enhance the distribution of the ss-siRNA to tissues other than the liver (Figure 6F).

Next, we determined the in vivo potency of the C16 ss-siRNA (29) (Figure 6B). The ss-siRNA 29 reduced the PTEN mRNA in a dose-dependent manner and exhibited a 3-fold greater in vivo potency compared to the unconjugated ss-siRNA 27 (Figure 6B). The increase in potency observed for the C16 ss-siRNA (29) compared to ss-siRNA (27) is more remarkable given that the in vitro potency of the ss-siRNA 29 was 10-fold lower compared to the ss-siRNA 27 (Figure 5A). Further increase in potency was observed for the ss-siRNA 29 following a longer-term dosing regime of twice a week for 3 weeks using either subcutaneous or intravenous administration (Figure 7A). Comparable potencies were observed for the ss-siRNA 29 using either route of administration (Figure 7A).

Finally, throughout the course of the in vivo studies, the animals were monitored for signs of ss-siRNA-associated toxicities. No adverse effects, such as elevated transaminase, bilirubin, cholesterol, and triglyceride levels or increased spleen and liver weights, were observed (Figures 7B and 7C).

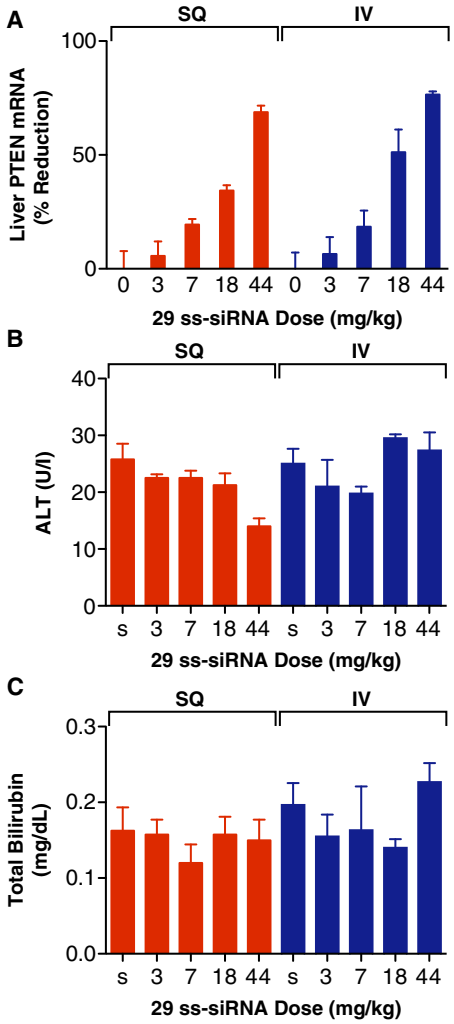


**Figure 7. In Vivo Activities of Modified ss-siRNAs following Multiple-Dose Administration**

(A) Dose-dependent reduction of PTEN mRNA from liver of mice (n = 4) treated with ss-siRNA 29 by either subcutaneous (red bars, SQ) or intravenous (blue bars, IV) administration. The ss-siRNA was dosed twice a week for 3 weeks, and the doses reported are per injection.

(B and C) Aminotransferase (B) and bilirubin (C) levels from the mice described in (A) treated with the ss-siRNA 29 by either subcutaneous (red bars) or intravenous (blue bars) administration.

Data are represented as mean ± SD.

## DISCUSSION

In this study, we identified single-strand siRNAs that reduce target mRNA in animals absent lipid formulation. We show that the ss-siRNA reduced the target mRNA both in vitro and in vivo by recruiting the RISC endoribonuclease Ago2 to cleave the mRNA (Figures 4A, 4C, and 6A). Importantly, we show that the 5′ phosphate is required for ss-siRNA activity, but not for siRNA activity, and as a result, metabolically stable 5′ phosphate analogs are necessary for ss-siRNA activity in vivo (Figures 4B and 4C). In fact, the structure-activity relationships observed for siRNAs differ sufficiently from ss-siRNAs, as to provide little guidance in designing effective ss-siRNAs (Figures 1C and 4B). Nor was the use of cellular homogenates or serum predictive of the robust nuclease and phosphatase activities found in animals (Figure 1C). In the end, identification of the optimum ss-siRNA required understanding the structure-activity relationships of human Ago2 activity, intrinsic potency, nuclease stability, and pharmacokinetics of the ss-siRNA.

### ss-siRNAs Activate RNAi in Cells and Animals

Our results demonstrate that the sense strand of siRNA is not required to activate RNAi in cells or animals (Figures 1C, 5A, and 5B). Ultimately, the RNAi mechanism requires the removal of the sense strand in order for the antisense strand of the siRNA to bind the mRNA target. Previous reports suggest that this occurs prior to binding human Ago2, as the enzyme was shown to bind single-stranded oligonucleotides, but not double-stranded oligonucleotides, and human Ago2 cleavage activity was observed only when the antisense strand was allowed to bind to the enzyme prior to the mRNA (Figure 2A) (Lima et al., 2009a).

As a component of the RISC-loading complex, Dicer is believed to participate in the translocation of siRNA to the RISC complex, which contains Ago2 (Chendrimada et al., 2005). Human Dicer has been shown to bind ss-siRNAs-containing purines at the 3′ terminus with affinities comparable to double-stranded siRNAs (Lima et al., 2009b; Kini and Walton, 2007; Macrae et al., 2006). Consistent with these observations, a 4-fold increase in potency was observed for ss-siRNAs containing an adenosine dinucleotide at the 3′ terminus (Figure 1C). Importantly, no statistically significant increase in human Ago2 cleavage activity was observed for the ss-siRNA containing the additional adenosine dinucleotide, suggesting that Ago2 was not contributing to the enhanced potency and that other factors (e.g., human Dicer) may be involved. Taken together, these results suggest that identifying additional contributors to the activities of ss-siRNAs and optimizing ss-siRNAs to better interact with these factors should further enhance the potencies of ss-siRNAs.

### A Metabolically Stable 5′ Phosphate Is Required for ss-siRNA Activity In Vivo

The identification of a potent and metabolically stable 5′ phosphate was paramount to achieving ss-siRNAs activity in vivo. Absent a 5′ phosphate, ss-siRNAs were inactive in vitro and in vivo (Figures 3C, 4B, and 5B). The 5′ methylenephophonate analogs were resistant to dephosphorylation in vivo, and those exhibiting a conformation and sterioelectronic properties similar to natural phosphate (e.g., 5′-*(E)*-vinylphosphonate) were more potent (Figures 5A and 5B). The 5′ phosphate was not required for activities of siRNAs (Figure 4B). Therefore, the loss of in vitro activity observed for the ss-siRNA without a 5′ phosphate suggests that the 5′ phosphate may play an additional role in the activities of ss-siRNAs.

### Discovering Potent and Metabolically Stable ss-siRNAs

In total, the results presented here provide a blueprint for designing metabolically stable ss-siRNAs capable of activating the RNAi mechanism in animals (Figure 1A). The 2′-F appears

to be unique in that it is tolerated and can be positioned anywhere within the ss-siRNA (Figure 1C). Unfortunately the ss-siRNAs containing 2′-F modifications exhibited poor nuclease stability and may, in part, explain the lack of in vivo activity reported for ss-siRNAs containing the 2′-F (Figure 1C) (Haringsma et al., 2012). Interestingly, these same ss-siRNAs administered in a lipid formulation were shown to exhibit in vivo activity, although the authors concluded that the mechanism of action was not Ago2-mediated degradation of the target mRNA (Haringsma et al., 2012).

The 2′-OMe and 2′-MOE modifications exhibit greater metabolic stability; however, excessive substitutions within the ss-siRNA are poorly tolerated (Lima et al., 2009a; Prakash et al., 2005). Alternating the 2′-F and 2′-OMe modifications in the ss-siRNAs enhanced the in vitro potency but required PS substitutions for enhanced metabolic stability (Figures 1A and 1C). Through the course of these studies, we enhanced the in vitro potency of the ss-siRNAs ~20-fold and metabolical stability to achieve a tissue half-life of 10 days and duration of action of ~7 days in mice (Figures 1A, 6C, and 6D).

## Enhancing the Pharmacokinetic Properties of ss-siRNAs

As demonstrated here, PS modifications can enhance not only metabolic stability of the ss-siRNA, but also the binding of oligonucleotides to serum proteins, which is essential to prevent rapid clearance of the oligonucleotides by glomerular filtration (Crooke, 2008). Optimal serum protein binding was observed with oligonucleotides containing >16 PS linkages (Crooke, 2008). Thus, it is not surprising that ss-siRNAs containing 14 PS were more rapidly cleared in vivo, reducing the distribution to peripheral tissues. Divided doses that reduce peak serum concentrations and renal clearance enhanced distribution to the liver somewhat, but adding lipophilic modification like C16 that enhance serum protein binding and cellular uptake was a better solution (Figures 5B, 5C, and 6F) (Crooke, 2008; Graham et al., 1998; Graham et al., 2001). These results suggest that further optimization of the nature and placement of the lipophilic modification should result in more potent ss-siRNAs.

## Implications for RNAi-Based Therapeutics and RNAi

Our results demonstrate that ss-siRNAs function as potent inhibitors of gene expression in animals and provide an alternative strategy for therapeutic gene silencing. ss-siRNAs offer several advantages over double-stranded RNAs. The need for just one strand also removes the risk that the passenger strand or its metabolites might cause undesirable off-target effects. Perhaps most importantly, double-stranded siRNA therapeutics requires lipid formulations to achieve useful levels of activity in vivo, further increasing the complexity and cost of manufacture and the potential for unanticipated toxicities. By contrast, ss-siRNAs achieve potent in vivo repression of gene expression using simple saline dosing solutions. Compared to double-stranded RNAs or antisense oligonucleotides, little has been done to optimize the activity of ss-siRNAs, and it is expected that further modification will enhance their value as therapeutics.

An example of the value of this approach is provided by the companion study in this issue examining allele-selective inhibition of huntingtin (HTT) expression (Yu et al., 2012). This study describes potent and allele-selective silencing. Importantly, allele-selective inhibition is achieved throughout the brains of mice following continuous infusion of ss-siRNA, demonstrating the potential for ss-siRNAs to modulate the expression of key genes in the central nervous system.

RNAi is almost always associated with duplex RNA. Reports of active single strands have been confined to assays in cell-free systems or limited descriptions of relatively inefficient activity in cells. Our data with ss-siRNAs demonstrate that potent gene silencing does not require duplex RNA and that the passenger strand is dispensable. The guide strand alone is sufficient to form interactions with RISC. Unlike duplex RNA, ss-siRNAs do require 5′ phosphates, identifying one key mechanistic difference between their actions. Our identification of a stable 5′ phosphate modification recognizes this difference and provides a route to efficient silencing in animals.

## EXPERIMENTAL PROCEDURES

### Synthesis of 5′-MP and 5′-VP ss-siRNAs

ssRNA were synthesized on ABI 394 synthesizer (1–2 μmol scale) or on GE Healthcare Bioscience ÄKTA oligopilot synthesizer (40–200 μmol scale) by the phosphoramidite coupling method on an UnyLinker solid support (Guzaev and Manoharan, 2003) packed in the column. A 0.1 M solution of 2′-F, 2′-*O*-Me, and 2′-*O*-MOE nucleoside phosphoramidites (1–3; Extended Experimental Procedures; Figure S1) in anhydrous $CH_3CN$ was used for the synthesis. The 2′-*O*-MOE-5-methyl uridine-5′-deoxy-5′-methylenephosphonate-3′-phosphoramidite (7; Figure S1), 2′-*O*-MOE-5-methyluridine-5′-deoxy-5′-vinylphosphonate-3′-phosphoramidite (8; Figure S1), 2′-*O*-[*N*-(decanoyl)-6-aminohexyl]-5-methyluridine-3′-phosphoramidite (9a; Figure S1), and 2′-*O*-[*N*-(hexadecanoyl)-6-aminohexyl]-5-methyluridine-3′-phosphoramidite (9b, please see Figure S1) were dissolved in 40% anhydrous dichloromethane in anhydrous $CH_3CN$ (0.15 M) and used for the synthesis. For the coupling step, the phosphoramidites were delivered 4- to 6-fold excess over the loading on the solid support, and phosphoramidite condensation was carried out for 10 min. A solution of 6% dichloroacetic acid in toluene was used for removing dimethoxytrityl (DMT) group from the 5′ hydroxyl group of the nucleotide. Extended detritylation condition was used to remove the DMT group from the secondary hydroxyl group of the UnyLinker solid support. 4,5-Dicyanoimidazole (0.7 M) in anhydrous $CH_3CN$ was used as activator during coupling step. Phosphorothioate linkages were introduced using 0.2 M solution of phenylacetyl disulfide in 1:1 pyridine/$CH_3CN$ as sulfur transfer reagent and were treated for 3 min except for the coupling of 5′-deoxy-5′methylenephosphonate and 5′-deoxy-5′-vinylphosphonate phosphoramidites (7 and 8; Figure S1); phosphorothioate linkages were introduced using a solution of 3-((dimethylaminomethylene)amino)-3*H*-1,2,4-dithiazole-5-thione (0.05 M, DDTT) in 1:1 pyridine/$CH_3CN$ and a 3 min contact. Solid-support-bound ssRNAs were washed with $CH_2Cl_2$ and dried under high vacuum for 4 hr. The ssRNAs were suspended in a solution of iodotrimethylsilane and pyridine in dichloromethane (dissolve 0.75 ml iodotrimethylsilane and 0.53 ml pyridine in 28.2 ml $CH_2Cl_2$, use 0.5 ml per μmol of solid support) and allowed to shake at room temperature for 30 min. Reaction was quenched with 50% triethylamine in $CH_3CN$ containing 1 M 2-mercaptoethanol (0.5 ml per μmol of solid support). Supernatant was decanted and the solid support washed with 1:1 triethylamine/$CH_3CN$ containing 1 M 2-mercaptoethanol (2 × 0.5 ml per μmol of solid support). A solution of 1:1 triethylamine/$CH_3CN$ containing 1M 2-mercaptoethanol (0.5 ml per μmol of solid support) was added and kept at room temperature for 45 min. Supernatant was decanted, and the residue aqueous ammonia (28–30 WT%) containing 1M 2-mercaptoethanol (0.75 ml per μmol of solid support) was added and heated at 55°C for 2 hr. The reaction mixture was allowed to come to room temperature and was kept for an additional 24 hr. The solid support was filtered and washed thoroughly with water. The filtrate and the washing were combined together

and then cooled in an ice bath and neutralized with glacial acetic acid. Resulting colloidal solution was allowed to stand at −20°C for 2–3 hr. The precipitate formed was collected by centrifugation followed by decanting the supernatant. The precipitated ssRNAs were then dissolved in water and purified by high-pressure liquid chromatography on a reverse phase column (Waters X-Bridge C-18 5 μm, 19 × 250 mm, A = 5 mM tributylammonium acetate in 5% aqueous $CH_3CN$, B = $CH_3CN$, 0 to 90% B in 80 min, flow 7 ml $min^{-1}$, λ = 260 nm). The fractions were analyzed by LC-MS, and fractions containing full-length ssRNAs were pooled together. The tributylammonium counter ions were exchanged to sodium by high-pressure liquid chromatography on a strong anion exchange column (GE Healthcare Bioscience, Source 30Q, 30 μm, 2.54 × 8 cm, A = 100 mM ammonium acetate in 30% aqueous $CH_3CN$, B = 1.5 M NaBr in A, 0%–40% of B in 60 min, flow 14 ml $min^{-1}$, λ = 260 nm). Desalting by HPLC on a reverse-phase column gave ssRNAs in an isolated yield of 15%–30% based on the initial loading on the solid support. ssRNAs were characterized by ion-pair-HPLC-coupled MS analysis with Agilent 1100 MSD system (Tables S1 and S2).

### Cleavage Activity for Recombinant Human GST-Ago2

Recombinant human Ago2 and $^{32}P$-labeled target RNA were prepared as described elsewhere (Lima et al., 2009b). Ago2 cleavage activity was carried out as described in Extended Experimental Procedures. The errors reported for the cleavage activities are based on three trials.

### In Vitro Potency of ss-siRNAs and siRNAs in Primary Hepatocytes

In vitro potency of ss-siRNAs and siRNAs was evaluated in primary hepatocytes following the protocol described in Extended Experimental Procedures.

### In Vitro Potency of ss-siRNA and siRNA in Transfected HeLa Cells

ss-siRNAs were transfected to HeLa cells using Lipofectamine 2000 (see Extended Experimental Procedures). Reduction of target mRNA was determined by qRT-PCR as previously described (Vickers et al., 2009). Target mRNA levels were normalized to total RNA using RiboGreen (Life Technologies). $IC_{50}$ curves and values were generated using Prism 4 software (GraphPad,).

### In Vivo Activity of ss-siRNA in Mice

Animal experiments were conducted according to American Association for the Accreditation of Laboratory Animal Care guidelines and were approved by the Animal Welfare Committee (see Extended Experimental Procedures). Mice were dosed by single0administration (n = 4) intravenous or subcutaneous injection, with the exception of subcutaneous doses >50 mg/kg, which consisted of subdivided injections of 25 mg/kg twice a day for the indicated number of days. Mice were sacrificed 48 hr posttreatment. Liver, kidney, and spleen weights were taken, and liver tissue was homogenized in guanidine isothiocyanate (Life Technologies) containing 8% β-mercaptoethanol (Sigma) immediately following the sacrifice. Reduction of target mRNA expression was determined by qRT-PCR as previously described (Vickers et al., 2009). Target mRNA levels were normalized to cyclophilin levels, and values were confirmed by RiboGreen (see Extended Experimental Procedures).

### 5′-RACE

Male Balb/c mice were subcutaneously injected with 25 mg/kg ssiRNA every 2 hr for a combined dose of 100 mg/kg. Animals were sacrificed 6 hr after final injection. Liver tissue was homogenized and purified as described above. RNA ligase-mediated rapid amplification of cDNA ends (5′-RACE) (Life Technologies) was performed on 1 ug of purified total RNA following manufacturer's instructions. PCR products were cloned using Topo TA-Mach1-T1 cells (Life Technologies), as directed by manufacturer's protocol. DNA was purified (QIAGEN) from cultured colonies and sequenced.

### Determination of ssRNA Liver Concentrations by Hybridization-Dependent Nuclease ELISA

Levels of ss-siRNAs in the liver of treated animals were determined using hybridization-dependent nuclease ELISA assay (see Extended Experimental Procedures).

### Determination of Tissue Concentrations and Metabolites of ssRNAs Using LC/MS

ss-siRNAs were extracted from livers and analyzed by liquid-chromatography-coupled mass spectroscopy analysis (see Extended Experimental Procedures). Mass measurements were made online using a single quadrupole mass spectrometer scanning 1000–2100 *m/z* in the negative ionization mode. Molecular masses were determined using ChemStation analysis package (Agilent, Santa Clara, CA). Manual evaluation was performed by comparing a table of calculated *m/z* values corresponding to potential metabolites with the peaks present in a given spectrum. Peak areas from extracted ion chromatograms were determined for ssRNAs, 3′ N-1 metabolites, and internal standard (Int. Std.), and a trendline was established using the calibration standards, plotting concentration of ssRNA against the ratio of the peak areas ssRNA. Internal standard concentration of ssRNAs and 3′ N-1 metabolites in study samples were determined using established trendlines and were reported as ug/g tissue.

## SUPPLEMENTAL INFORMATION

Supplemental Information includes Extended Experimental Procedures, five figures, and two tables and can be found with this article online at http://dx.doi.org/10.1016/j.cell.2012.08.014.

## ACKNOWLEDGMENTS

We thank Dr. C. Frank Bennett, Prof. David R. Corey, Dongbo Yu, Rachel Meyers, and Muthiah Manoharan for helpful discussion. We also thank Dr. Balkrishen Bhat, Charles A. Allerson, and Andres Berdeja for their initial contribution for this work and Prof. Gregory Hannon for the Ago2 knockout cells.

Received: March 22, 2012
Revised: May 31, 2012
Accepted: August 8, 2012
Published: August 30, 2012

## REFERENCES

Allerson, C.R., Sioufi, N., Jarres, R., Prakash, T.P., Naik, N., Berdeja, A., Wanders, L., Griffey, R.H., Swayze, E.E., and Bhat, B. (2005). Fully 2′-modified oligonucleotide duplexes with improved in vitro potency and stability compared to unmodified small interfering RNA. J. Med. Chem. *48*, 901–904.

Bennett, C.F., and Swayze, E.E. (2010). RNA targeting therapeutics: molecular mechanisms of antisense oligonucleotides as a therapeutic platform. Annu. Rev. Pharmacol. Toxicol. *50*, 259–293.

Bernstein, E., Caudy, A.A., Hammond, S.M., and Hannon, G.J. (2001). Role for a bidentate ribonuclease in the initiation step of RNA interference. Nature *409*, 363–366.

Braasch, D.A., Jensen, S., Liu, Y., Kaur, K., Arar, K., White, M.A., and Corey, D.R. (2003). RNA interference in mammalian cells by chemically-modified RNA. Biochemistry *42*, 7967–7975.

Caplen, N.J. (2003). RNAi as a gene therapy approach. Expert Opin. Biol. Ther. *3*, 575–586.

Chen, P.Y., Weinmann, L., Gaidatzis, D., Pei, Y., Zavolan, M., Tuschl, T., and Meister, G. (2008). Strand-specific 5′-O-methylation of siRNA duplexes controls guide strand selection and targeting specificity. RNA *14*, 263–274.

Chendrimada, T.P., Gregory, R.I., Kumaraswamy, E., Norman, J., Cooch, N., Nishikura, K., and Shiekhattar, R. (2005). TRBP recruits the Dicer complex to Ago2 for microRNA processing and gene silencing. Nature *436*, 740–744.

Crooke, S.T. (2008). Antisense Drug Technology: Principles, Strategies, and Applications, Second Edition (Boca Raton, FL: CRC Press).

Dande, P., Prakash, T.P., Sioufi, N., Gaus, H., Jarres, R., Berdeja, A., Swayze, E.E., Griffey, R.H., and Bhat, B. (2006). Improving RNA interference in mammalian cells by 4′-thio-modified small interfering RNA (siRNA): effect on siRNA activity and nuclease stability when used in combination with 2′-O-alkyl modifications. J. Med. Chem. *49*, 1624–1634.

Elbashir, S.M., Lendeckel, W., and Tuschl, T. (2001). RNA interference is mediated by 21- and 22-nucleotide RNAs. Genes Dev. *15*, 188–200.

Fire, A., Xu, S., Montgomery, M.K., Kostas, S.A., Driver, S.E., and Mello, C.C. (1998). Potent and specific genetic interference by double-stranded RNA in Caenorhabditis elegans. Nature *391*, 806–811.

Graham, M.J., Crooke, S.T., Monteith, D.K., Cooper, S.R., Lemonidis, K.M., Stecker, K.K., Martin, M.J., and Crooke, R.M. (1998). In vivo distribution and metabolism of a phosphorothioate oligonucleotide within rat liver after intravenous administration. J. Pharmacol. Exp. Ther. *286*, 447–458.

Graham, M.J., Crooke, S.T., Lemonidis, K.M., Gaus, H.J., Templin, M.V., and Crooke, R.M. (2001). Hepatic distribution of a phosphorothioate oligodeoxynucleotide within rodents following intravenous administration. Biochem. Pharmacol. *62*, 297–306.

Guzaev, A.P., and Manoharan, M. (2003). A conformationally preorganized universal solid support for efficient oligonucleotide synthesis. J. Am. Chem. Soc. *125*, 2380–2381.

Hall, A.H., Wan, J., Shaughnessy, E.E., Ramsay Shaw, B., and Alexander, K.A. (2004). RNA interference using boranophosphate siRNAs: structure-activity relationships. Nucleic Acids Res. *32*, 5991–6000.

Haringsma, H.J., Li, J.J., Soriano, F., Kenski, D.M., Flanagan, W.M., and Willingham, A.T. (2012). mRNA knockdown by single strand RNA is improved by chemical modifications. Nucleic Acids Res. *40*, 4125–4136.

Holen, T., Amarzguioui, M., Babaie, E., and Prydz, H. (2003). Similar behaviour of single-strand and double-strand siRNAs suggests they act through a common RNAi pathway. Nucleic Acids Res. *31*, 2401–2407.

Kini, H.K., and Walton, S.P. (2007). In vitro binding of single-stranded RNA by human Dicer. FEBS Lett. *581*, 5611–5616.

Lima, W.F., Wu, H., Nichols, J.G., Sun, H., Murray, H.M., and Crooke, S.T. (2009a). Binding and cleavage specificities of human Argonaute2. J. Biol. Chem. *284*, 26017–26028.

Lima, W.F., Murray, H., Nichols, J.G., Wu, H., Sun, H., Prakash, T.P., Berdeja, A.R., Gaus, H.J., and Crooke, S.T. (2009b). Human Dicer binds short single-strand and double-strand RNA with high affinity and interacts with different regions of the nucleic acids. J. Biol. Chem. *284*, 2535–2548.

Macrae, I.J., Zhou, K., Li, F., Repic, A., Brooks, A.N., Cande, W.Z., Adams, P.D., and Doudna, J.A. (2006). Structural basis for double-stranded RNA processing by Dicer. Science *311*, 195–198.

Martinez, J., Patkaniowska, A., Urlaub, H., Lührmann, R., and Tuschl, T. (2002). Single-stranded antisense siRNAs guide target RNA cleavage in RNAi. Cell *110*, 563–574.

Meister, G., Landthaler, M., Patkaniowska, A., Dorsett, Y., Teng, G., and Tuschl, T. (2004). Human Argonaute2 mediates RNA cleavage targeted by miRNAs and siRNAs. Mol. Cell *15*, 185–197.

Nykänen, A., Haley, B., and Zamore, P.D. (2001). ATP requirements and small interfering RNA structure in the RNA interference pathway. Cell *107*, 309–321.

Prakash, T.P., Allerson, C.R., Dande, P., Vickers, T.A., Sioufi, N., Jarres, R., Baker, B.F., Swayze, E.E., Griffey, R.H., and Bhat, B. (2005). Positional effect of chemical modifications on short interference RNA activity in mammalian cells. J. Med. Chem. *48*, 4247–4253.

Rand, T.A., Ginalski, K., Grishin, N.V., and Wang, X. (2004). Biochemical identification of Argonaute 2 as the sole protein required for RNA-induced silencing complex activity. Proc. Natl. Acad. Sci. USA *101*, 14385–14389.

Rivas, F.V., Tolia, N.H., Song, J.J., Aragon, J.P., Liu, J., Hannon, G.J., and Joshua-Tor, L. (2005). Purified Argonaute2 and an siRNA form recombinant human RISC. Nat. Struct. Mol. Biol. *12*, 340–349.

Rose, S.D., Kim, D.-H., Amarzguioui, M., Heidel, J.D., Collingwood, M.A., Davis, M.E., Rossi, J.J., and Behlke, M.A. (2005). Functional polarity is introduced by Dicer processing of short substrate RNAs. Nucleic Acids Res. *33*, 4140–4156.

Schwarz, D.S., Hutvágner, G., Haley, B., and Zamore, P.D. (2002). Evidence that siRNAs function as guides, not primers, in the Drosophila and human RNAi pathways. Mol. Cell *10*, 537–548.

Song, J.J., Smith, S.K., Hannon, G.J., and Joshua-Tor, L. (2004). Crystal structure of Argonaute and its implications for RISC slicer activity. Science *305*, 1434–1437.

Tao, W., Mao, X., Davide, J.P., Ng, B., Cai, M., Burke, P.A., Sachs, A.B., and Sepp-Lorenzino, L. (2011). Mechanistically probing lipid-siRNA nanoparticle-associated toxicities identifies Jak inhibitors effective in mitigating multifaceted toxic responses. Mol. Ther. *19*, 567–575.

Tomari, Y., Matranga, C., Haley, B., Martinez, N., and Zamore, P.D. (2004). A protein sensor for siRNA asymmetry. Science *306*, 1377–1380.

Vaishnaw, A.K., Gollob, J., Gamba-Vitalo, C., Hutabarat, R., Sah, D., Meyers, R., de Fougerolles, T., and Maraganore, J. (2010). A status report on RNAi therapeutics. Silence *1*, 14.

Wu, H., MacLeod, A.R., Lima, W.F., and Crooke, S.T. (1998). Identification and partial purification of human double strand RNase activity. A novel terminating mechanism for oligoribonucleotide antisense drugs. J. Biol. Chem. *273*, 2532–2542.

Yu, D., Pendergraff, H., Liu, J., Kordasiewicz, H., Cleveland, D.W., Swayze, E.E., Lima, W.F., Crooke, S.T., Prakash, T.P., and Corey, D.R. (2012). Single-stranded RNAs use RNAi to potently and allele-selectively inhibit mutant huntingtin expression. Cell *150*, this issue, 895–908.